iScience

CellPress

Article

Functional Modulation of Gene Expression by Ultraconserved Long Non-coding RNA TUC338 during Growth of Human Hepatocellular Carcinoma

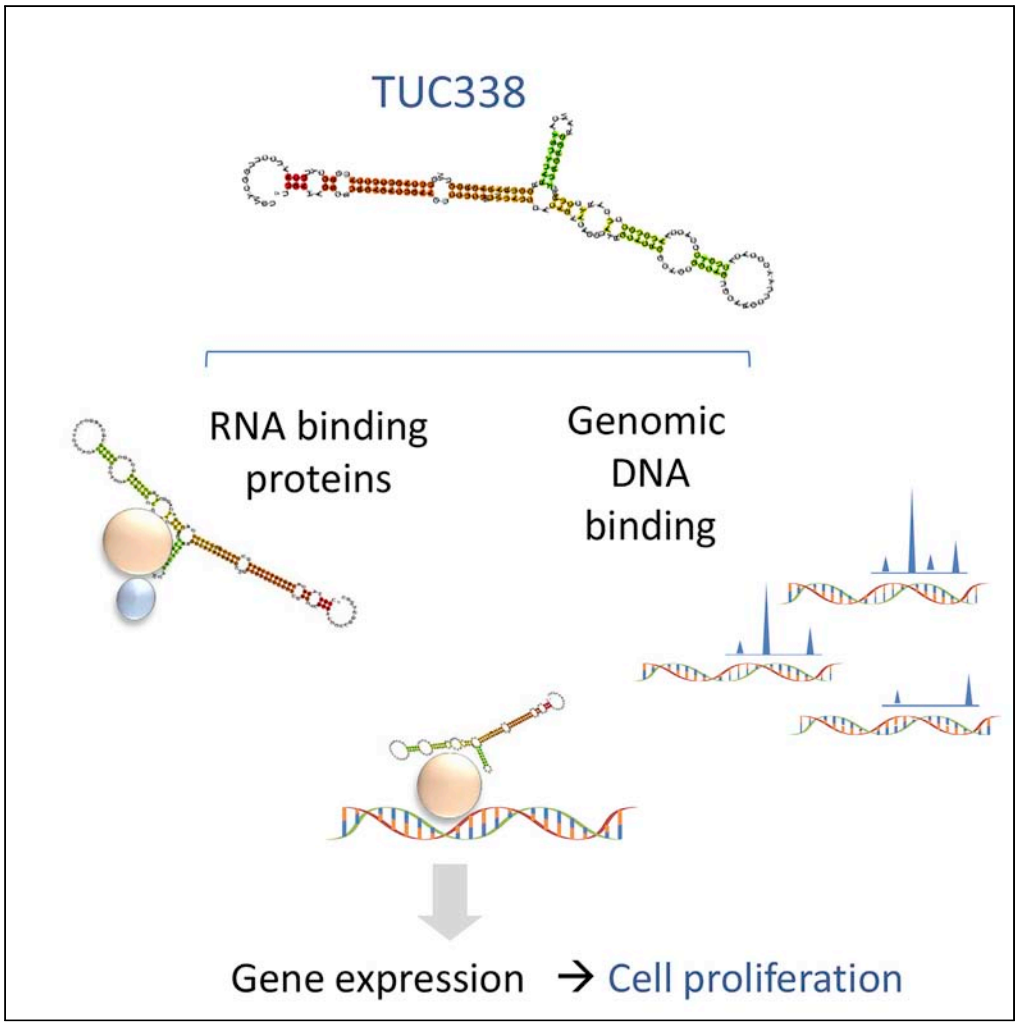

Hui-Ju Wen, Michael P. Walsh, Irene K. Yan, Kenji Takahashi, Alan Fields, Tushar Patel

patel.tushar@mayo.edu

HIGHLIGHTS

TUC338 can modulate cell proliferation by sequence-specific genomic binding

TUC338 binds to motifs homologous to those of the tumor suppressors Pax6 and p53

Plasminogen activator inhibitor-1 mRNA binding protein is a TUC338-binding protein

TUC338 can regulate PAI-RBP1 target gene plasminogen activator inhibitor-1

Wen et al., iScience *2*, 210–220
April 27, 2018
https://doi.org/10.1016/j.isci.2018.03.004

iScience

CellPress

Article

Functional Modulation of Gene Expression by Ultraconserved Long Non-coding RNA TUC338 during Growth of Human Hepatocellular Carcinoma

Hui-Ju Wen,[1,2] Michael P. Walsh,[2] Irene K. Yan,[1,2] Kenji Takahashi,[1,2] Alan Fields,[2] and Tushar Patel[1,2,3,*]

SUMMARY

TUC338 is an ultraconserved long non-coding RNA that contributes to transformed cell growth in hepatocellular carcinoma (HCC). Genomic regions of TUC338 occupancy were enriched in unique or known binding motifs homologous to the tumor suppressors Pax6 and p53. Genes involved in cell proliferation were enriched within a 9-kb range of TUC338-binding sites. TUC338 RNA-based purification was used to isolate chromatin for mass spectrometry, and the plasminogen activator inhibitor-1 RNA-binding protein (PAI-RBP1) was identified as a TUC338 RNA-binding partner. The PAI-RBP1 target gene plasminogen activator inhibitor-1 (PAI-1) itself could also be post-transcriptionally regulated by TUC338. Thus modulation of transformed cell growth by TUC338 may involve binding to PAI-RBP1 as well as to sequence-defined *cis*-binding sites to modulate gene expression. These findings suggest that ultraconserved RNAs such as TUC338 can function in a manner analogous to transcription factors to modulate cell proliferation and transformed cell growth in HCC.

INTRODUCTION

A large portion of the non-protein coding regions of the human genome has been shown to be actively transcribed into RNA molecules (Costa, 2010; Ponting and Belgard, 2010). A subgroup of this transcribed non-coding RNA genome consists of long non-coding RNA, i.e., with nucleotide sequences >200 bp, which include ultraconserved elements that are fully conserved across human and rodent genomes (Bejerano et al., 2004; Calin et al., 2007). The molecular function of these transcribed ultraconserved RNAs (ucRNAs) is unknown. Although many long non-coding RNAs lack primary sequence conservation across species, ucRNAs are highly conserved, suggesting an important evolutionarily conserved biological function for transcribed ucRNAs (Katzman et al., 2007). Indeed, ucRNA expression has been shown to occur in a tissue-specific manner, and aberrant expression of ucRNAs has been noted in several types of cancers, such as chronic lymphocytic leukemias, colorectal carcinoma, and hepatocellular carcinomas (HCCs) (Braconi et al., 2011; Calin et al., 2007; Sana et al., 2012). Scaruffi et al. also discovered 28 ucRNAs associated with good outcome in patients diagnosed with metastatic neuroblastoma (Scaruffi et al., 2009). Given these findings, some ucRNAs may have functional roles that are of relevance to cancer diagnosis, prognosis, or treatment response.

HCC is the major primary liver cancer and the third leading cause of cancer-related death worldwide. We have previously identified a striking expression of uc.338 in HCC and cloned the transcript encoding this ultraconserved element as a long non-coding RNA, TUC338. Modulation of TUC338 expression resulted in altered expression of several genes and transformed cell growth in human and mouse hepatocytes (Braconi et al., 2011). Understanding the molecular basis of these actions may provide new insights into the molecular functions of the transcribed ucRNA as well as identify therapeutic targets for HCC. Thus the aim of this study was to understand the mechanisms by which TUC338 could regulate the expression of genes that could contribute to transformed cell growth in HCC.

A number of long non-coding RNAs (lncRNAs) have been revealed to associate with nuclear factors to form long non-coding RNA-ribonucleoproteins (RNPs) that may function as transcriptional activators or repressors for gene expression. In addition, it is believed that long non-coding RNAs are able to recruit the chromatin-modifying complex to specific genomic loci. Findings from these previous studies of long non-coding RNAs raise the possibility that TUC338 may function in HCC by associating with its protein partners and/or selective regions of the genome to mediate its biological effects. Thus we performed chromatin isolation

[1]Department of Transplantation, Mayo Clinic, 4500 San Pablo Road, Jacksonville, FL 32224, USA

[2]Department of Cancer Biology, Mayo Clinic, Jacksonville, FL 32224, USA

[3]Lead Contact

*Correspondence: patel.tushar@mayo.edu

https://doi.org/10.1016/j.isci.2018.03.004

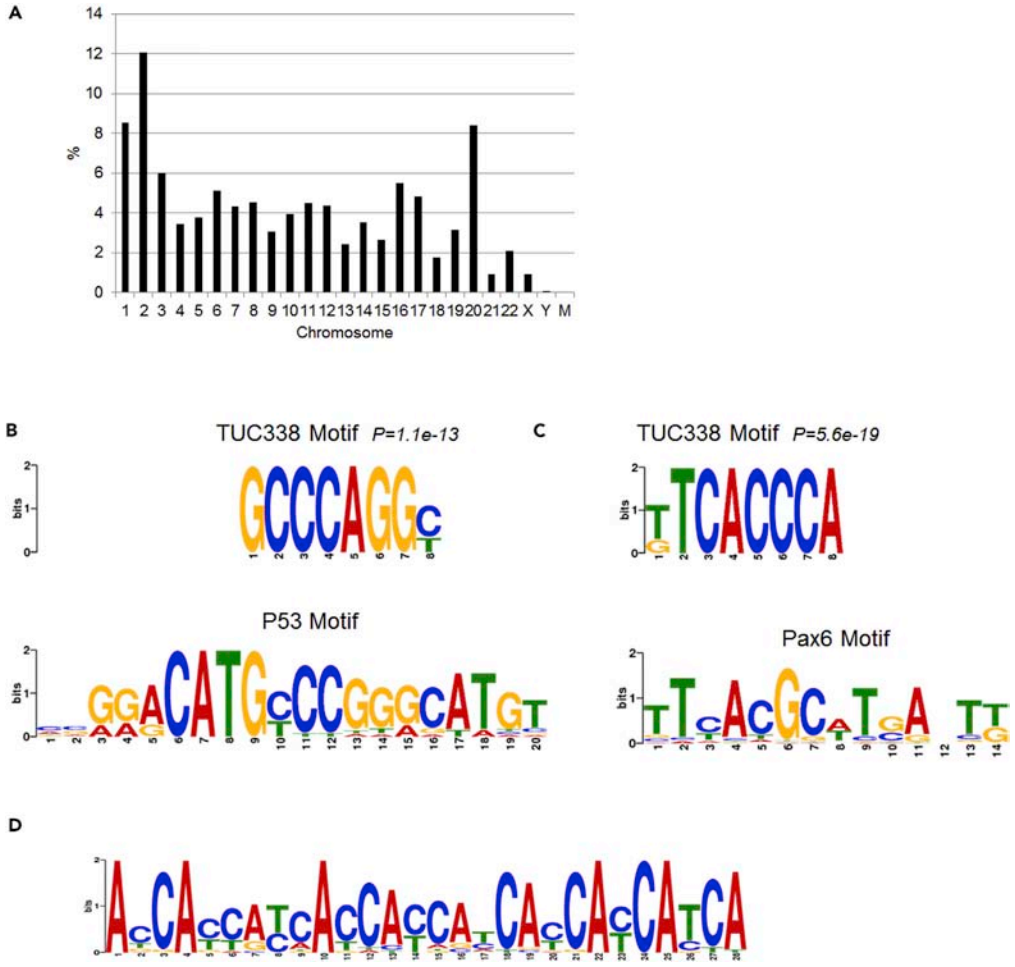

Figure 1. Genomic Binding Sites of TUC338

(A) Chromosome distribution of TUC338-binding sites derived from 2,469 true TUC338 peaks identified by sequencing of TUC338 RNA-bound chromatin.

(B and C) Homology of an enriched binding site motif with (B) p53 and (C) Pax 6 motifs from the Jaspar core database.

(D) Unique TUC338-binding site motif.

by RNA purification followed by mass spectrometry and genomic analysis to identify TUC338-binding proteins and TUC338 occupancy sites throughout the genome.

RESULTS

Chromatin-Binding Sites of TUC338

In order for long non-coding RNA to modulate gene expression, access to chromatin is required. We postulated that binding to DNA would be important for TUC338 function and sought to identify and analyze the genomic binding sites of TUC338 RNA. Two non-overlapping sets of biotinylated TUC338 RNA-binding probes were used as affinity reagents for chromatin precipitation from HepG2 cells (see Table S1). This was followed by high-throughput sequencing to identify DNA bound to the pooled TUC338 RNA probes in each of the two pooled probe sets (see Transparent Methods). We analyzed data that were obtained only from both probe sets and excluded all data obtained from any one probe set alone. This approach avoids any potential effects of direct or indirect off-target hybridization. TUC338 RNA chromatin immunoprecipitation (IP) peaks could be distinguished from nonspecific background based on the strength of the TUC338 RNA IP signals. We excluded sharp peaks of <600 bp because these could be artifacts. Because the probe sets do not show any overlap, artifactual identification of peaks with motifs homologous to those of probe sets is also avoided. Examination of RNA occupancy regions using model-based analysis of ChIP-seq

		Count	p Value	FDR
1	GO:0046578~regulation of Ras protein signal transduction	12	0.005403	8.8404
2	GO:0006729~tetrahydrobiopterin biosynthetic process	3	0.006402	10.3927
3	GO:0035272~exocrine system development	4	0.007187	11.5937
4	GO:0046146~tetrahydrobiopterin metabolic process	3	0.008838	14.0722
5	GO:0050679~positive regulation of epithelial cell proliferation	5	0.010974	17.1819

Table 1. Enriched Genes within Short Range (9 kb) of TUC338-Binding Sites
Gene ontology analysis was performed for biological processes using DAVID. The top five ontologies are listed.
FDR, false discovery rate.

(MACS) (Zhang et al., 2008) identified 2,469 high-TUC338-occupancy regions in the genome. These TUC338-binding regions were identified in all chromosomes, with the greatest number being in chromosome 2 (Figure 1). These data indicate that there are several TUC338 RNA occupancy sites and that these are focal and non-randomly distributed across the genome.

Sequence Specificity of Binding Sites

These observations suggest that TUC338 may bind to specific sequences. To understand how TUC338 may be targeted to specific regions in the chromatin and to determine the role of potential sequence-specific binding sites in targeting TUC338 complexes, we analyzed the sequence of the 2,469 TUC338-binding sites by Multiple EM for Motif Elicitation (MEME) (Machanick and Bailey, 2011).

Motif analysis revealed that 110 TUC338-binding sites were enriched for a motif ($p = 1.1 \times 10^{-13}$) that is homologous to the p53-binding motif (Figure 1B). To examine the potential effect of TUC338 on p53 binding at these sites, we analyzed p53 activation in response to TUC338 knockdown using small interfering RNA (siRNA) to TUC338 and observed a 31% $\pm$ 6% increase in p53 activity. In addition, other transcription-factor-binding motifs were also identified. For example, 107 TUC338-binding sites were enriched for a motif ($p = 5.6 \times 10^{-19}$) that is homologous to the Pax6-binding motif (Figure 1C). In addition, other unique TUC338 binding motifs were also identified (Figure 1D). The motifs lacked homology with the ultraconserved sequence. Consequently, genomic binding interactions may be unrelated to factors that determine sequence ultraconservation.

Analysis of *cis*-Genes Associated with TUC338-Binding Sites

We next examined the genomic locations of all TUC338-binding regions to identify neighboring genes that could be *cis*-regulated by TUC338. A total of 3,306 potential target genes were identified within 1,000 kb of the 2,469 TUC338-binding sites. Of these potential targets, 404 were located within 9 kb of gene loci, and gene ontology analysis showed highly significant enrichment of TUC338-associated gene loci involved in cell proliferation (Table 1), distinct from those genes located at a further distance (Table 2). Of the 18 genes associated with cell proliferation, 9 have been functionally linked to HCC: E2F1 (Chen et al., 2012), BOP1 (Chung et al., 2011), CYR61 (Feng et al., 2008), EGFR (Huether et al., 2005), ERCC1 (Fautrel et al., 2005),

		Count	p Value	FDR
1	GO:0000902~cell morphogenesis	109	4.19×10^{-11}	7.94×10^{-8}
2	GO:0000904~cell morphogenesis involved in differentiation	80	6.37×10^{-10}	1.21×10^{-6}
3	GO:0030182~neuron differentiation	123	9.72×10^{-10}	1.84×10^{-6}
4	GO:0006928~cell motion	130	1.86×10^{-9}	3.52×10^{-6}
5	GO:0035295~tube development	73	2.16×10^{-9}	4.09×10^{-6}

Table 2. Enriched Genes within Long Range (9–1000 kb) of TUC338-Binding Sites
Gene ontology analysis was performed for biological processes using DAVID. The top five ontologies are listed.
FDR, false discovery rate.

Gene Symbol	Gene Name	Reported Roles in HCC
E2F1	E2F transcription factor 1	Associated with worse outcomes in patients with HCC
MXD1	MAX dimerization protein 1	
STIL	SCL/TAL1 interrupting locus	
SH2D2A	SH2 domain protein 2A	
BOP1	Block of proliferation 1	Oncogene role in HCC invasiveness and metastasis
CCKBR	Cholecystokinin B receptor	
CYR61	Cysteine-rich, angiogenic inducer, 61	Tumor suppressor role in HCC
DAB2	Disabled homolog 2, mitogen-responsive phosphoprotein	
EGFR	Epidermal growth factor receptor	Predictive marker for HCC metastasis and recurrence
EMP2	Epithelial membrane protein 2	
ERCC1	Excision repair cross-complementing rodent repair deficiency, complementation group 1	Overexpression is associated with liver fibrogenesis and HCC
FOXC1	Forkhead box C1	Overexpression promotes metastasis in HCC
GFI1B	Growth-factor-independent 1B transcription repressor	
LAMA5	Laminin, alpha 5	
OSM	Oncostatin M	Overexpression is associated with HCC development
PES1	Pescadillo homolog 1, containing BRCT domain	
SHH	Sonic hedgehog homolog	Overexpression is associated with size and invasion of HCC
ZEB2	Zinc finger E-box binding homeobox 2	Tumor suppressor role in HCC

Table 3. Enriched Genes within a Short Range of TUC338-Binding Sites and Associated with Cell Proliferation in Hepatocellular Cancer

FOXC1 (Xia et al., 2012), OSM (Liang et al., 2012), SHH (Chen et al., 2010), and ZEB2 (Cai et al., 2012) (Table 3). Enrichment was also noted for genes involved in Ras signal transduction, tetrahydrobiopterin and pteridine metabolic process, exocrine system development, and actin filament organization. Potential long-range interactions between target genes and TUC338-binding sites were also analyzed for the 2,979 genes identified between 9 kb and 1 Mb of TUC338-binding sites. Gene ontology analysis of this gene set revealed significant enrichment of genes involved in cell proliferation as well as cell morphogenesis and differentiation, neuron differentiation, cell motion, and DNA-dependent transcriptional regulation (Table 2). Experimentally, modulation of TUC338 using siRNA in HCC cells alters the expression of several genes. Using Affymetrix GeneChip mRNA analysis, we identified 611 genes that are altered in expression by greater than 2-log-fold in response to TUC338 knockdown. TUC338-binding sites were identified within 1,000 kbp of the gene loci for 89 of these genes, indicating the potential for their direct regulation by TUC338. Functional annotation analysis of these 89 genes using DAVID identified that the most highly significant enrichment occurred for genes involved in biological processes related to cell proliferation. TUC338 has been shown to modulate HCC cell proliferation. Thus these data suggest that *cis*-regulation of expression of genes involved in aberrant cell proliferation could represent a mechanism by which TUC338 contributes to tumor growth in HCC.

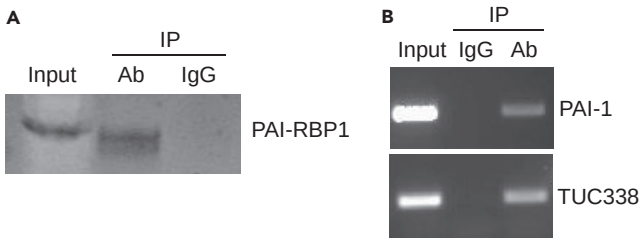

Figure 2. Association of TUC338 with PAI-RBP1 and PAI-1 RNA

RNA immunoprecipitation was performed using a monoclonal PAI-RBP1 antibody (Ab) or mouse IgG (IgG) to immunoprecipitate PAI-RBP1 and RNA complex from HepG2 cell lysates.

(A) Western blot was performed using anti-PAI-RBP1 antibody.

(B) TUC338 and PAI-1 were amplified from RNA immunoprecipitates by RT-PCR using TUC338- and PAI-1-specific primers.

Identification of PAI-RBP1 as a TUC338-Binding Protein

Binding at target sites can occur either via direct hybridization or in association with other factors such as proteins or other RNAs. None of the binding sites that were identified by our analyses showed homology to TUC338, making it unlikely that TUC338 RNA binding occurred by direct hybridization. Thus we sought to identify proteins that would bind to TUC338. As with studies to identify DNA-binding sites, two independent pools of biotinylated oligonucleotide probes that were complementary to separate regions of TUC338 without any overlapping sequences were hybridized to TUC338 RNA in HepG2 cell lysates. The proteins that were pulled down were then separated and analyzed by nano-high-pressure liquid chromatography (HPLC)-electrospray tandem mass spectrometry. Potential protein binding partners to TUC338 RNA were identified as proteins that were pulled down by both independent probe sets. The plasminogen activator inhibitor-1 RNA-binding protein (PAI-RBP1) isoform 2 was identified as a TUC338 RNA-binding protein. To verify these findings, we performed RNA immunoprecipitation using monoclonal PAI-RBP1 antibody (Figure 2A) and confirmed that PAI-RBP1 is a TUC338 RNA-binding protein. PAI-RBP1 was initially identified as an RNA-binding protein that could post-transcriptionally regulate plasminogen activator inhibitor-1 (PAI-1) expression (Heaton et al., 2001, 2003). Indeed, enrichment of PAI-1 mRNA (Figure 2B, upper panel) was noted with PAI-RBP1 antibody compared with control IgG antibody pull-down. Furthermore, enrichment of TUC338 was also observed using the PAI-RBP1 antibody but not the IgG antibody (Figure 2B, bottom panel). These data show that PAI-RBP1 can bind to PAI-1 mRNA as well as to TUC338 RNA.

Aberrant Expression of PAI-RBP1 in Malignant Hepatocytes Regulated by TUC338

To examine the biological correlates of TUC338 binding, we next evaluated PAI-RBP1 mRNA expression in malignant (HepG2 and Huh7) and non-malignant (HH) human hepatocytes. We found that PAI-RBP1 mRNA expression was increased in the malignant hepatocytes (Figure 3), similar to the increased expression of TUC338 observed in malignant hepatocytes (Braconi et al., 2011; Calin et al., 2007; Sana et al., 2012). The relationship between expression of PAI-RBP1 and TUC338 was further studied. Knockdown of TUC338 using siRNA in HepG2 cells decreased both PAI-RBP1 mRNA and protein (Figure 3). The knockdown efficiency of TUC338 was confirmed by real-time PCR. Thus PAI-RBP1 expression is positively regulated by TUC338. Moreover, knockdown of PAI-RBP1 using siRNA resulted in a reduction in TUC338 RNA expression. However, knockdown of PAI-RBP1 did not alter the effect of the siRNA to TUC338 on p53 activation. Because PAI-RBP1 is a PAI-1-binding protein, we next examined the effect of TUC338 on the regulation of PAI-1 expression. PAI-1 mRNA and protein expression were examined following siRNA-mediated TUC338 knockdown in HepG2 cells. Compared with cells transfected with control non-targeting (NT) siRNA, a reduction in PAI-1 mRNA as well as in secreted PAI-1 protein was noted in cells transfected with siRNA to TUC338 (Figures 3E and 3F).

TUC338 Regulates PAI-1 Expression by Modulating the 3′ UTR of the 2.2-kb Transcript

To examine the effects of TUC338 on PAI-1 expression, we first examined the PAI-1 promoter sequence and identified several putative TUC338-binding motifs in the 5′ UTR. However, PAI-1 was not identified among the genes that are candidates for direct regulation by TUC338 binding, suggesting that the regulation of PAI-1 expression did not occur via direct transcriptional activation. Two transcripts of human PAI-1 mRNA (3.2 and 2.2 kb) have been reported, and these differ only in the length of their 3′ UTR (Fattal and Billadello,

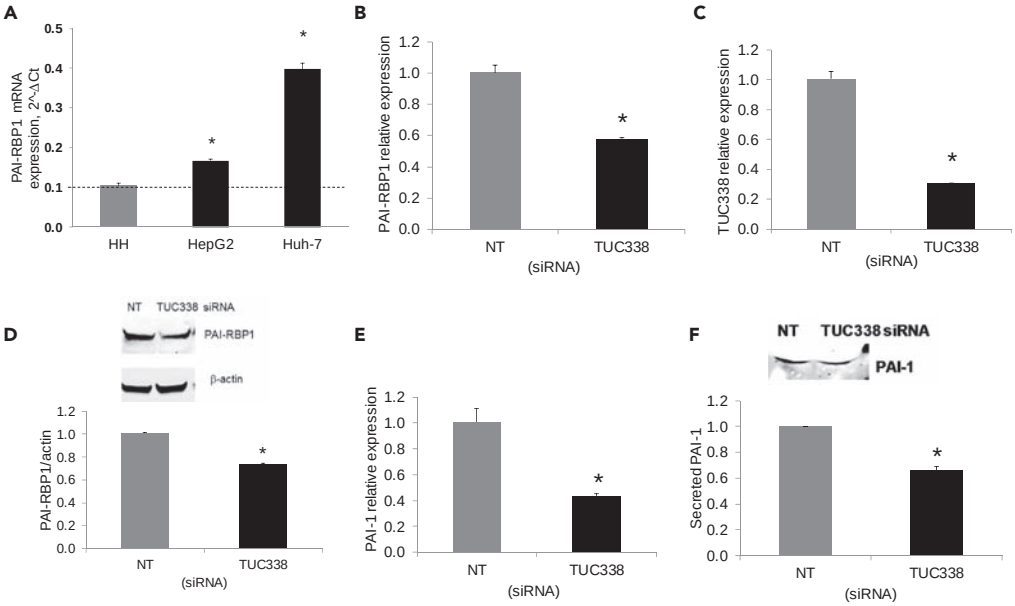

Figure 3. TUC338 Positively Regulates PAI-RBP1 and PAI-1 Expression

(A) PAI-RBP1 mRNA level in non-malignant (HH) or malignant (HepG2, HUH-7) hepatocytes was assessed by reverse transcription followed by SYBR green real-time PCR and normalized by GAPDH. Values are mean ± SE (n = 3, *p < 0.01). (B–E) HepG2 cells were transfected with non-targeting (NT) siRNA or siRNA against TUC338. The RNA expression levels of PAI-RBP1 (B) and TUC338 (C) were measured by SYBR green real-time PCR and normalized to GAPDH. (D) The protein expression of PAI-RBP1 and β-actin was determined by western blot. Values are mean ± SE of the fold over NT (n = 3, *p < 0.01). (E) The mRNA expression level of PAI-1 was measured by SYBR green real-time PCR and normalized to GAPDH.
(F) PAI-1 protein secreted in the media was determined by western blot. Values are mean ± SE of the fold over NT (n = 3, *p < 0.01).

1993). We cloned the two 3′ UTRs of the 3.2- and 2.2-kb transcripts into pGL3 vector to generate the reporter constructs PAI-13U and PAI-13US, respectively (Figure 4A), and examined the response of 3′ UTR activation to TUC338 knockdown. Compared with control NT siRNA, the siRNA to TUC338 decreased PAI-13US and slightly increased PAI-13U activity (Figure 4B). Furthermore, PAI-13US activity was increased by the expression of full-length TUC338, further demonstrating the effect of TUC338 on the 3′ UTR of the 2.2-kb PAI-1 transcript (Figure 4C). These results suggest that TUC338 upregulates PAI-1 expression by stabilizing the 2.2-kb PAI-1 transcript.

Identification of Sites of Interaction between PAI-RBP1 and TUC338 RNA

We next sought to define the PAI-RBP1-interacting regions of the TUC338 RNA by electrophoretic mobility shift assay (EMSA) using HepG2 cell extracts and full-length or truncated TUC338 RNA fragments. First, the full-length TUC338 RNA was labeled with biotin at the 3′ end and incubated with binding buffer either alone or with HepG2 cell extracts (Figure 5A, lanes 1–4). A high-molecular-weight shift band was observed in the presence of cell extract. Binding increased with the concentration of full-length TUC338 RNA probes and was reduced by the addition of excess unlabeled TUC338 RNA (Figure 5A, lanes 3–6). Furthermore, the addition of PAI-RBP1 antibody confirmed the specificity of binding of TUC338 to PAI-RBP1 (Figure 5A, lane 7). RNA EMSA was then performed using five truncated biotin-labeled TUC338 RNA probes. After incubation with cell extract, strong binding was observed with TUC338/1–115, 116–237, 238–354, and 461–575 but not with TUC338/355–460 (Figure 5B). The specificity of binding was confirmed by using unlabeled homologous RNA oligonucleotides. In addition, all of the binding involved PAI-RBP1 protein as it was reduced by the addition of PAI-RBP1 antibody (Figure 5C). These results indicate that TUC338 associates with PAI-RBP1 through the regions nt 1–354 and nt 461–575 of TUC338.

PAI-RBP1 Modulates Transformed Cell Growth of Human Hepatocytes

TUC338 modulates transformed cell growth in hepatocytes. To further evaluate the contribution of the TUC338-binding protein PAI-RBP1 to biological effects, we next assessed the impact of PAI-RBP1

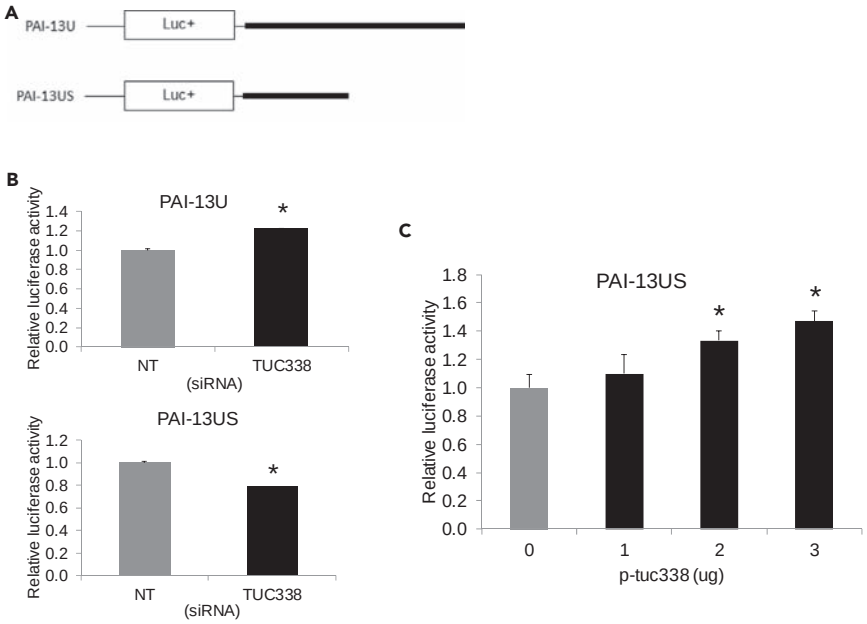

Figure 4. TUC338 Regulates the Activity of 3′ UTR of 2.2 kb PAI-1 mRNA

(A) PAI-1 3′ UTR (solid black box) was cloned into pGL3-control vector downstream of the firefly luciferase gene. PAI-13U contains the 3′ UTR of 3.2- kb PAI-1 mRNA. PAI-13US contains the 3′ UTR of 2.2 kb PAI-1 mRNA.

(B) After 24-hr transfection of siRNAs against non-targeting (NT) or TUC338, HepG2 cells were co-transfected with the *Renilla* luciferase reporter vector and the firefly luciferase reporter construct (PAI-13U or PAI-13US). After another 24 hr, luciferase assay was performed.

(C) HepG2 cells were co-transfected with PAI-13US construct, the *Renilla* luciferase reporter vector, and pcDNA3.1 empty vector or pcDNA3.1 containing full-length TUC338 (p-tuc338). Luciferase assay was performed at 24 hr post transfection. The firefly luciferase activities were normalized to the *Renilla* luciferase activities.

Values are mean ± SE of the fold over NT or pcDNA3.1 empty vector (n = 3, *p < 0.05).

knockdown on cell proliferation in HepG2 cells. Knockdown efficiency of PAI-RBP1 was confirmed by real-time PCR (Figure 6A). HepG2 cell viability was unchanged by PAI-RBP1 knockdown compared with NT controls (Figure 6B). However, compared with control NT siRNA, siRNA to PAI-RBP1 decreased anchorage-independent cell growth of HepG2 HCC cells, assessed using two complementary assays to evaluate growth in soft agar (Figure 6C) as well as by a clonogenic growth assay (Figure 6D). These studies verify the contribution of PAI-RBP1 to transformed cell growth in human hepatocytes.

DISCUSSION

TUC338 is a long non-coding RNA that is capable of modulating gene expression and transformed cell growth in hepatocytes. Chromatin immunoprecipitation using pools of biotinylated probes with non-overlapping sequence complementarity to TUC338 RNA followed by genomic sequencing enabled us to localize specific loci at which TUC338 RNA can bind. We identified multiple genomic TUC338-binding sites; some of these are similar to sites associated with known transcription factors. Because TUC338 RNA can bind to these sites, it is likely that these loci are involved in TUC338 function. There are some limitations of this approach. Different loci may be enriched with differing levels of efficiency, for example, if there is restricted access to the genomic site. Moreover, enrichment but not the stoichiometry of binding at a specific genomic locus is identified, and thus the molecular basis of the interaction between TUC338 and these loci is unknown.

In prior studies, we have observed an increase in nuclear TUC338 in human HCC, raising the possibility that TUC338 may be involved in chromatin remodeling to facilitate gene expression. The greatest number of TUC338-binding sites occurs on chromosome 2, and two of the most significantly enriched sites of TUC338 occupancy are homologous to the binding sites of Pax6 and p53. p53 can bind to DNA as a tetramer, in a sequence-specific manner, and can regulate gene transcription (Vazquez et al., 2008). Owing

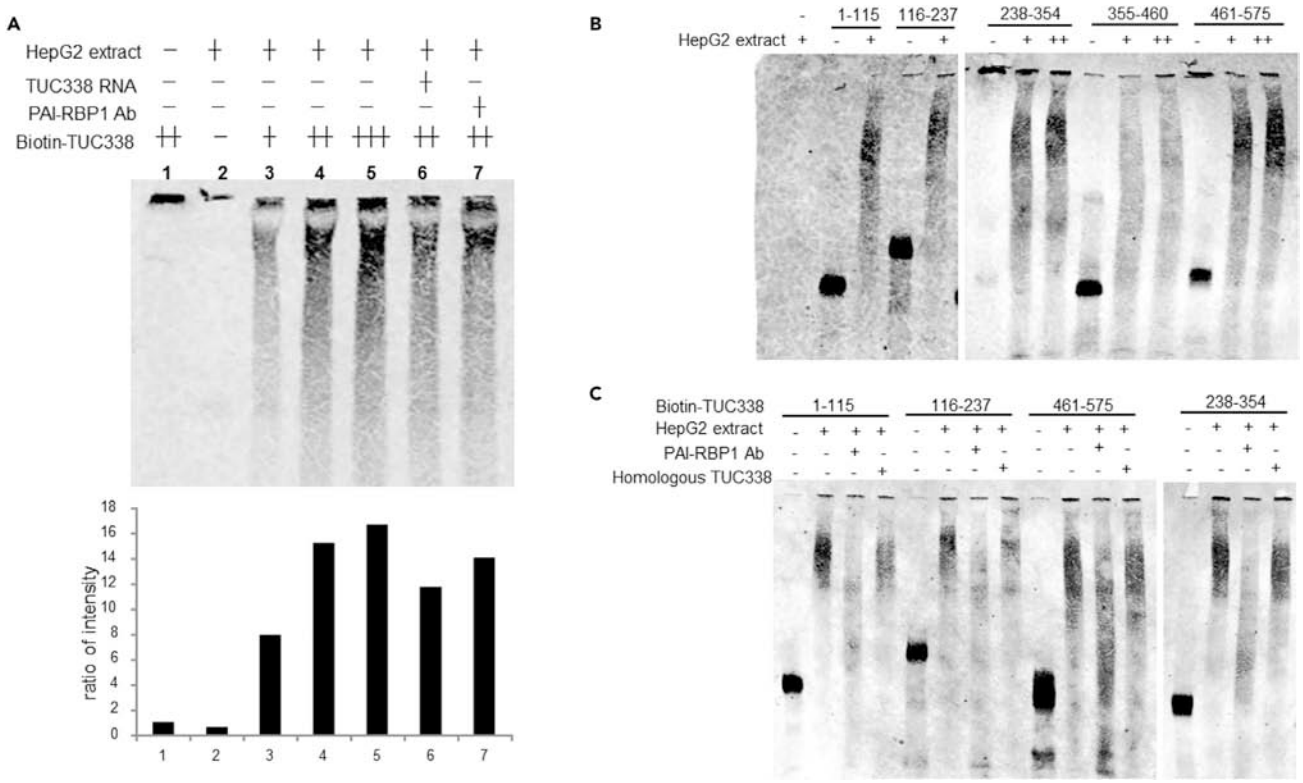

Figure 5. *In Vitro* Interaction of TUC338 and PAI-RBP1 Protein by RNA EMSA

(A) Full-length TUC338 RNA labeled at the 3′ end was used as the RNA probe (Biotin-TUC338) and incubated with cell lysate extracted from HepG2 cells. Full-length TUC338 RNA and PAI-RBP1 antibody served as competitors. The signal was quantified by NIH Image software.

(B and C) Five truncated Biotin-TUC338 (1–115, 116–237, 238–354, 355–460, 461–575) were used as RNA probes. The unlabeled truncated RNA homologous to the labeled truncated RNA was used as a specific competitor (Homologous TUC338).

to the high similarity between the binding motifs of TUC338 and p53, competition for binding to DNA could occur between TUC338 and p53. Thus the increased expression of TUC338 could result in sequestration of p53 from DNA binding at these sites, functionally silencing the p53 target genes. Similar effects could also occur at other motifs such as Pax6. In addition to its role in development and cell differentiation, Pax6 transcriptionally regulates the genes involved in cell growth and apoptosis (Mayes et al., 2006; Shyr et al., 2010) and can act as a tumor suppressor. Thus a potential mechanism of action of TUC338 could involve interference with binding of tumor suppressors to target DNA with suppression of downstream transcription. Similar to the mechanisms reported for regulatory properties of other long non-coding RNAs (Rinn and Chang, 2012), we speculate that TUC338 could act as a guide to route transcription factors to specific genomic loci, which in turn activate or represses gene expression, or alternatively as a scaffold for the interaction between specific binding proteins and molecular complexes, resulting in chromatin remodeling.

The lack of sequence homology to TUC338 among the enriched occupancy sites indicates that direct binding through sequence-based hybridization is unlikely and supports the involvement of additional factors such as RNA-binding proteins or other RNAs that could serve to recruit and facilitate TUC338 RNA binding at these enriched target sites. To identify TUC338 RNA-binding proteins, a similar approach was used in which TUC338 RNA was enriched and co-purified proteins were identified by mass spectrometry. This approach to identify binding proteins is the converse of an RNA immunoprecipitation study in which proteins are first pulled down and RNA-binding partners identified. Proteomic analysis identified PAI-RBP1 as an RNA-binding protein that could bind to TUC338 and contribute to transformed cell growth. PAI-RBP1 contributes to post-transcriptional regulation of PAI-1 mRNA by binding to PAI-1 mRNA 3′ UTR, and we further demonstrated that TUC338 can regulate PAI-1 mRNA through its 3′ UTR. The lack of any complementary sequence between PAI-1 3′ UTR and TUC338 RNA supports

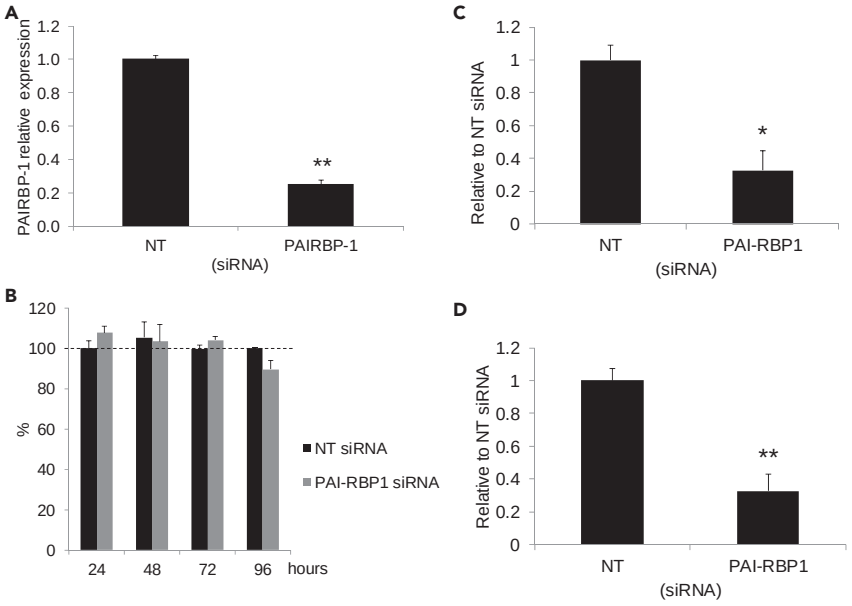

Figure 6. PAI-RBP1 RNAi Affects Anchorage-Independent Growth

HepG2 cells were transfected with non-targeting (NT) or PAI-RBP1 siRNA.

(A) The RNA expression levels of TUC338 were measured by SYBR green real-time PCR and normalized to GAPDH.

(B) At 24 hr post transfection, cells were plated in 96-well plates. Cell proliferation was assessed at indicated time points.

(C) At 24 hr post transfection, cells were plated in 96-well plates with soft agar. After 1 week, anchorage-independent growth was assessed fluorometrically.

(D) At 24 hr post transfection, cells were plated in 24-well plates with soft agar. After 4 weeks, cell colonies were stained with Giemsa and counted.

Values are mean ± SE of the fold over NT ($n = 3$, $^{*}p < 0.01$, $^{**}p < 0.005$).

the involvement of RNA-binding proteins in post-transcriptional regulation instead of direct complementary binding of TUC338 to PAI-1 3′ UTR.

Further indirect evidence that TUC338 can interact with RNA-binding proteins is provided by the results of the EMSA studies. PAI-RBP1 can bind to rat PAI-1 mRNA 3′ UTR at the cyclic nucleotide responsive sequence (CRS), which comprises A- and U-rich sequences (Heaton et al., 2001). AUUUA and UUAUUUAUU motifs are targets of RNA-binding proteins, and we identified several A- and U-rich regions in the TUC338 sequence. Use of truncated TUC338 RNA probes and EMSA revealed that the only region unable to form protein complexes (between nucleotides 355 and 460) also lacks A-rich, U-rich, and AUUUA sequences.

Biological roles for PAI-RBP1 and PAI-1 in tumor progression have been postulated. PAI-RBP1 expression is increased in several different cancers, such as ovarian, prostate, and lung cancer, and, moreover, correlates with advanced stage of ovarian cancer (Koensgen et al., 2007; Sun et al., 2012). Likewise, an increased expression of PAI-1 has also been shown in many solid tumors, including HCC, and is associated with poor patient prognosis (Berger, 2002; Koensgen et al., 2007; Zhou et al., 2000). In addition to post-transcriptional regulation, PAI-RBP1 has a nuclear function associated with chromatin remodeling based on its interaction with proteins such as chromodomain helicase DNA-binding protein 3 (CHD3) (Lemos et al., 2003). Although CHD3 was not identified as a TUC338-binding protein in our studies, it remains possible that the complex of TUC338 and PAI-RBP1 could be involved in gene regulation through chromatin remodeling.

These results showing the pervasive genomic nature of TUC338 RNA occupancy emphasize a broad role in gene regulation. More specifically, there is evidence that direct physical interactions between TUC338 RNA and PAI-RBP1 resulting in post-transcriptional regulation of PAI-1 mRNA could contribute, in part, to the oncogenic effects of enhanced TUC338 expression that is observed in HCC. These observations provide

new insights and will generate new hypotheses into understanding the dynamic mechanisms by which the ucRNA TUC338 modulates gene expression, which will be helpful to understand the effects of this long non-coding RNA in tumorigenesis.

METHODS

All methods can be found in the accompanying Transparent Methods supplemental file.

SUPPLEMENTAL INFORMATION

Supplemental Information includes Transparent Methods and one table and can be found with this article online at https://doi.org/10.1016/j.isci.2018.03.004.

ACKNOWLEDGMENTS

Financial support: Supported in part by Grant DK069370 from the National Institutes of Health.

AUTHOR CONTRIBUTIONS

H.-J.W. and T.P. conceived the experiments and wrote the article. H.-J.W., I.K.Y., and K.T. conducted the experiments and M.P.W. performed data analysis. A.F. provided expertise and feedback. T.P. provided support.

DECLARATION OF INTERESTS

The authors declare no competing interests.

Received: December 10, 2017
Revised: February 7, 2018
Accepted: February 14, 2018
Published: March 22, 2018

REFERENCES

Bejerano, G., Pheasant, M., Makunin, I., Stephen, S., Kent, W.J., Mattick, J.S., and Haussler, D. (2004). Ultraconserved elements in the human genome. Science *304*, 1321–1325.

Berger, D.H. (2002). Plasmin/plasminogen system in colorectal cancer. World J. Surg. *26*, 767–771.

Braconi, C., Valeri, N., Kogure, T., Gasparini, P., Huang, N., Nuovo, G.J., Terracciano, L., Croce, C.M., and Patel, T. (2011). Expression and functional role of a transcribed noncoding RNA with an ultraconserved element in hepatocellular carcinoma. Proc. Natl. Acad. Sci. USA *108*, 786–791.

Cai, M.Y., Luo, R.Z., Chen, J.W., Pei, X.Q., Lu, J.B., Hou, J.H., and Yun, J.P. (2012). Overexpression of ZEB2 in peritumoral liver tissue correlates with favorable survival after curative resection of hepatocellular carcinoma. PLoS One *7*, e32838.

Calin, G.A., Liu, C.G., Ferracin, M., Hyslop, T., Spizzo, R., Sevignani, C., Fabbri, M., Cimmino, A., Lee, E.J., Wojcik, S.E., et al. (2007). Ultraconserved regions encoding ncRNAs are altered in human leukemias and carcinomas. Cancer Cell *12*, 215–229.

Chen, X.L., Cheng, Q.Y., She, M.R., Wang, Q., Huang, X.H., Cao, L.Q., Fu, X.H., and Chen, J.S. (2010). Expression of sonic hedgehog signaling components in hepatocellular carcinoma and cyclopamine-induced apoptosis through Bcl-2 downregulation in vitro. Arch. Med. Res. *41*, 315–323.

Chen, Y.L., Uen, Y.H., Li, C.F., Horng, K.C., Chen, L.R., Wu, W.R., Tseng, H.Y., Huang, H.Y., Wu, L.C., and Shiue, Y.L. (2012). The E2F transcription factor 1 transactives stathmin 1 in hepatocellular carcinoma. Ann. Surg. Oncol. *20*, 4041–4054.

Chung, K.Y., Cheng, I.K., Ching, A.K., Chu, J.H., Lai, P.B., and Wong, N. (2011). Block of proliferation 1 (BOP1) plays an oncogenic role in hepatocellular carcinoma by promoting epithelial-to-mesenchymal transition. Hepatology *54*, 307–318.

Costa, F.F. (2010). Non-coding RNAs: meet thy masters. Bioessays *32*, 599–608.

Fattal, P.G., and Billadello, J.J. (1993). Species-specific differential cleavage and polyadenylation of plasminogen activator inhibitor type 1 hnRNA. Nucleic Acids Res. *21*, 1463–1466.

Fautrel, A., Andrieux, L., Musso, O., Boudjema, K., Guillouzo, A., and Langouet, S. (2005). Overexpression of the two nucleotide excision repair genes ERCC1 and XPC in human hepatocellular carcinoma. J. Hepatol. *43*, 288–293.

Feng, P., Wang, B., and Ren, E.C. (2008). Cyr61/CCN1 is a tumor suppressor in human hepatocellular carcinoma and involved in DNA damage response. Int. J. Biochem. Cell Biol. *40*, 98–109.

Heaton, J.H., Dlakic, W.M., Dlakic, M., and Gelehrter, T.D. (2001). Identification and cDNA cloning of a novel RNA-binding protein that interacts with the cyclic nucleotide-responsive sequence in the Type-1 plasminogen activator inhibitor mRNA. J. Biol. Chem. *276*, 3341–3347.

Heaton, J.H., Dlakic, W.M., and Gelehrter, T.D. (2003). Posttranscriptional regulation of PAI-1 gene expression. Thromb. Haemost. *89*, 959–966.

Huether, A., Hopfner, M., Baradari, V., Schuppan, D., and Scherubl, H. (2005). EGFR blockade by cetuximab alone or as combination therapy for growth control of hepatocellular cancer. Biochem. Pharmacol. *70*, 1568–1578.

Katzman, S., Kern, A.D., Bejerano, G., Fewell, G., Fulton, L., Wilson, R.K., Salama, S.R., and Haussler, D. (2007). Human genome ultraconserved elements are ultraselected. Science *317*, 915.

Koensgen, D., Mustea, A., Klaman, I., Sun, P., Zafrakas, M., Lichtenegger, W., Denkert, C., Dahl, E., and Sehouli, J. (2007). Expression analysis and RNA localization of PAI-RBP1 (SERBP1) in epithelial ovarian cancer: association with tumor progression. Gynecol. Oncol. *107*, 266–273.

Lemos, T.A., Passos, D.O., Nery, F.C., and Kobarg, J. (2003). Characterization of a new family of proteins that interact with the C-terminal region of the chromatin-remodeling factor CHD-3. FEBS Lett. *533*, 14–20.

Liang, H., Block, T.M., Wang, M., Nefsky, B., Long, R., Hafner, J., Mehta, A.S., Marrero, J., Gish, R., and Norton, P.A. (2012). Interleukin-6 and oncostatin M are elevated in liver disease in conjunction with candidate hepatocellular carcinoma biomarker GP73. Cancer Biomark. *11*, 161–171.

Machanick, P., and Bailey, T.L. (2011). MEME-ChIP: motif analysis of large DNA datasets. Bioinformatics *27*, 1696–1697.

Mayes, D.A., Hu, Y., Teng, Y., Siegel, E., Wu, X., Panda, K., Tan, F., Yung, W.K., and Zhou, Y.H. (2006). PAX6 suppresses the invasiveness of glioblastoma cells and the expression of the matrix metalloproteinase-2 gene. Cancer Res. *66*, 9809–9817.

Ponting, C.P., and Belgard, T.G. (2010). Transcribed dark matter: meaning or myth? Hum. Mol. Genet. *19*, R162–R168.

Rinn, J.L., and Chang, H.Y. (2012). Genome regulation by long noncoding RNAs. Annu. Rev. Biochem. *81*, 145–166.

Sana, J., Hankeova, S., Svoboda, M., Kiss, I., Vyzula, R., and Slaby, O. (2012). Expression levels of transcribed ultraconserved regions uc.73 and uc.388 are altered in colorectal cancer. Oncology *82*, 114–118.

Scaruffi, P., Stigliani, S., Moretti, S., Coco, S., De Vecchi, C., Valdora, F., Garaventa, A., Bonassi, S., and Tonini, G.P. (2009). Transcribed-Ultra Conserved Region expression is associated with outcome in high-risk neuroblastoma. BMC Cancer *9*, 441.

Shyr, C.R., Tsai, M.Y., Yeh, S., Kang, H.Y., Chang, Y.C., Wong, P.L., Huang, C.C., Huang, K.E., and Chang, C. (2010). Tumor suppressor PAX6 functions as androgen receptor co-repressor to inhibit prostate cancer growth. Prostate *70*, 190–199.

Sun, W., Guo, C., Meng, X., Yu, Y., Jin, Y., Tong, D., Geng, J., Huang, Q., Qi, J., Liu, A., et al. (2012). Differential expression of PAI-RBP1, C1orf142, and COTL1 in non-small cell lung cancer cell lines with different tumor metastatic potential. J. Investig. Med. *60*, 689–694.

Vazquez, A., Bond, E.E., Levine, A.J., and Bond, G.L. (2008). The genetics of the p53 pathway, apoptosis and cancer therapy. Nat. Rev. Drug Discov. *7*, 979–987.

Xia, L., Huang, W., Tian, D., Zhu, H., Qi, X., Chen, Z., Zhang, Y., Hu, H., Fan, D., Nie, Y., et al. (2012). Overexpression of forkhead box C1 promotes tumor metastasis and indicates poor prognosis in hepatocellular carcinoma. Hepatology *57*, 610–624.

Zhang, Y., Liu, T., Meyer, C.A., Eeckhoute, J., Johnson, D.S., Bernstein, B.E., Nusbaum, C., Myers, R.M., Brown, M., Li, W., et al. (2008). Model-based analysis of chip-seq (MACS). Genome Biol. *9*, R137.

Zhou, L., Hayashi, Y., Itoh, T., Wang, W., Rui, J., and Itoh, H. (2000). Expression of urokinase-type plasminogen activator, urokinase-type plasminogen activator receptor, and plasminogen activator inhibitor-1 and -2 in hepatocellular carcinoma. Pathol. Int. *50*, 392–397.

ISCI, Volume *2*

Supplemental Information

Functional Modulation of Gene Expression by Ultraconserved Long Non-coding RNA TUC338 during Growth of Human Hepatocellular Carcinoma

Hui-Ju Wen, Michael P. Walsh, Irene K. Yan, Kenji Takahashi, Alan Fields, and Tushar Patel

Supplemental Information

Table S1. TUC RNA binding probes used for chromatin purification. Related to Figure 1 and Transparent Methods. The sequence of each biotinylated RNA binding oligo probe is shown. Probes were pooled into two separate sets, comprised of odd-number or even-number designated oligos respectively, and used for chromatin isolation.

TUC338-1: ttgaacccctacagagccca

TUC338-3: gggcaacagagctgatgcca

TUC338-5: tcacactgcacaattgggct

TUC338-7: cgagctgtaatcagtgaatt

TUC338-9: accttgtcaccagcatgaaa

TUC338-11: agactgaacatcccctctca

TUC338-13: tgttggcagtctcggctgag

TUC338-15: acaggtggtgtccacagcac

TUC338-17: cctgggtgaaatgaggttgg

TUC338-2: tcctggtcagtgtgggatta

TUC338-4: tttcaataagaatgaagggg

TUC338-6: aaaagttacctagtggcaga

TUC338-8: ggagctcagacacaatttga

TUC338-10: cctgtggataaatagaggat

TUC338-12: ggaaggattgagtgagcctt

TUC338-14: aaaatcaccagcgccactgg

TUC338-16: gggtcagtccaggtccccgt

TUC338-18: taccatctggtgggctacgc

Transparent Methods

Cell Culture condition and siRNA transfection.

HepG2 and Huh-7 cells were obtained from American Type Culture Collection (Manassas, VA) and maintained in Dulbecco's modified Eagle's medium /high glucose medium (Life technologies, Grand Island, NY) supplemented with 10% fetal bovine serum and 1% antibiotic antibiotic mix at 37°C with 5% CO_2. Gene specific siRNAs and non-targeting (NT) siRNA controls were designed using siDESIGN and obtained from Dharmacon (Rockford, IL) (Braconi et al., 2011). The sequence of PAI-RBP1 siRNA is 5'-UACCUCUUCAACUUCAUUCUU. The sequence of TUC338 siRNA was described previously (Braconi et al., 2011). HepG2 cells were transfected with siRNAs for 24 or 48 hours before further experiments. siRNA transfection was performed using lipofectamine 2000 (Life Technologies, Grand Island, NY) in 6-well plates.

RNA based purification for chromatin isolation.

Antisense 20 base-pair DNA probes were designed based on the full-length TUC338 sequence using Probe Designer (Biosearch Technologies) and compared with the human genome using the BLAST tool. Eighteen DNA oligonucleotides were selected, and grouped into two sets, an even numbered and an odd-numbered set based on their relative positions along the TUC338 sequence (Supplemental Table 1). All probes were generated with biotin-TEG at the 3'end (Gene Link, Hawthorne, NY). Isolation of TUC338 RNA bound proteins from HepG2 cell lysates was performed as described by Chu et al. (Chu et al., 2012, Chu et al., 2011).

Identification of TUC338 RNA binding proteins.

Protein identification was performed by the Mayo Proteomics Core Facility. Isolated proteins were digested with trypsin followed by analysis using nano high-pressure liquid chromatography electrospray tandem mass spectrometry. Peptide fragments were aligned to proteins using the Swissprot human protein database.

RNA sequencing and data analysis.

High throughput sequencing was performed by the Mayo Clinic DNA Sequencing Core Facility using Illumina MiSeq with read length of 51 bp. The GEO accession number for the RNA seq samples is GSE109490. Raw reads were mapped to reference human genome (hg19) using Bowtie (Langmead et al., 2009). The MACS algorithm was used to find true peaks, corresponding to high confidence binding sites of TUC338 as described, using thresholds of average coverage >1.5 and a Pearson correlation of 1 (Chu et al., 2011). TUC338 binding motifs were identified from these high confidence TUC338 binding sites using MEME-ChIP (Machanick and Bailey, 2011, Bailey, 2011). Alignments with known motifs were performed using TOMTOM and Jaspar and UniPROBE databases (Gupta et al., 2007). The annotations of nearby genes to these TUC338 binding sites were analyzed using GREAT version 2.0.2 (McLean et al., 2010), and Gene Ontology analyses of these genes was performed using DAVID (Huang da et al., 2009b, Huang da et al., 2009a).

RNA immunoprecipitation.

RNA immunoprecipitation was performed as described(Sun et al., 2006). Briefly, cells were lysed in SDS-lysis buffer supplemented with protease inhibitors cocktail and SUPERase-in (Life technologies, Grand Island, NY). Immunoprecipitation was performed using antibodies to PAI-RBP1 (Abnova, Taiwan) and mouse IgG (Santa Cruz Biotechnology, Santa Cruz, CA), with protein A/G agarose-plus (Santa Cruz Biotechnology, Santa Cruz, CA). Immunoprecipitates were used for either protein determination by western blot, or for RNA extraction and RT-PCR

Real-time PCR analysis.
Total cellular RNA was extracted from cells or immunoprecipitates using TRIzol reagent (Life Technologies, Grand Island, NY), treated with RNase-free DNaseI (Qiagen, Valencia, CA), and reverse-transcribed to cDNA using iScript cDNA synthesis kit (Bio-Rad Laboratories, Hercules, CA). Quantitative real-time PCR for PAI-RBP1, PAI-1 mRNA and TUC338 RNA, was performed using SYBR Advantage qPCR Premix (Clontech Laboratories, Mountain View, CA) and Mx3000p system (Stratagene, Santa Clara, CA). The following forward (F) and reverse (R) primers were used: TUC338 (F: 5'- AGCGACAGTGCGAGCTTT, R: 5'-GGAAGGATTGAGTGAGCCTT), GAPDH (F: 5'-GAGTCAACGGATTTGGTCGT, R: 5'-TTGATTTTGGAGGGATCTCG), PAI-RBP1 (F: 5'-ACCTATTCGAGGTCGTGGTG, R: 5'-TGGGGGACTCTGTTAATTCG), PAI-1 (F: 5'-GGGCCATGGAACAAGGATGA, R: 5'-CTCCTTTCCCAAGCAAGTTG). GAPDH was used as an internal control for mRNA expression.

Microarray analysis.
Gene expression microarray analysis was performed using the Human Exon 1.0 ST Array (Affymetrix) in RNA obtained from HepG2 cells transfected with LNA antisense oligonucleotides to TUC338 or controls and analyzed using XRAY software (Biotique Systems Inc.) as previously reported (Braconi et al., 2011). The GEO accession number for the dataset is GSE110259. Genes that were significantly differentially expressed were identified and then compared with Gene Ontology classifications to identify overrepresentation in groups of the molecular function, cell processes, or pathway classes. The input files were assigned to 2 groups: High UC (control) or low UC (LNA to TUC338), and were normalized with full quantile normalization. For each input array, for each probe expression value, the array ith percentile probe value was replaced with the average of all array ith percentile points. Next, the 5,359,576 probes were manipulated as follows. Probes with GC count less than 6 and greater than 17 were excluded from the analysis. Probe scores were then transformed by taking the Natural Logarithm of 0.1 plus the probe score. Each probe score was corrected for background by subtracting the median expression score of background probes with similar GC content. The array contained 1,404,693 probe-sets. The expression score for a probe-set was defined to be the median of its probe expression scores and probe-sets with fewer than 3 probes (that pass all of the tests defined below) were excluded from further analysis. Only 'Core' probe-sets that corresponded to high quality genomic features like RefSeq (www.ncbi.nlm.nih.gov) or Ensembl (www.ensembl.org) transcripts were analyzed. Non-expressed probe-sets and low-variance probe-sets were excluded from the analysis. The array contained a total of 312,368 transcript clusters. After the filters described above were applied 9,191 contained between 4 and 200 probe-sets. These were tested for differential gene expression using mixed model, nested analysis of variance. The data were analyzed with Analysis of Variance (ANOVA) and multiple tests correction was performed using the Benjamini and Hochberg False Discovery Rate. To establish the presence or absence of expression for a particular gene in a group, we derived a p-value to test the null hypothesis that the average of CEL files belonging to the group is not above background. 611 genes with significant gene expression differences between the groups ($p<0.01$) were identified. The false discovery rate was less than 1.00E-02 for differential gene expression tests.

Western blotting.
Conditioned media were collected and centrifuged at 10,000 rpm for 3 minutes. Cells were harvested by trypsinization and centrifugation at 3,000 rpm for 3 minutes. Cell pellets were resuspended in RIPA buffer (1% NP40, 0.1% SDS, 50mM Tris-HCl, 150mM NaCl, 0.5% sodium deoxycholate, 1mM EDTA, 1mM PMSF, proteinase inhibitor cocktail) and incubated at 4°C for 30 minutes. Gel electrophoresis was performed using equivalent amounts of proteins and NuPAGE 4%-12% Bis-Tris gels (Life Technologies, Grand Island, NY). Proteins were transferred to nitrocellulose membranes. The membranes were blocked with blocking buffer (LI-

COR Biosciences, Lincoln, NE) followed by incubation with primary antibodies and then IRDye680RD and IRDye800CW-labeled secondary antibodies (LI-COR Biosciences, Lincoln, NE). PAI-RBP1 antibody was purchased from Abnova. PAI-1 antibody and □-actin was purchased from Santa Cruz biotechnology. The protein of interest was visualized using the LI-COR Odyssey infrared imaging system (LI-COR Biosciences, Lincoln, NE) and quantitated by NIH ImageJ.

RNA electrophoretic mobility shift assay (EMSA).

RNA probes were made by cloning the full-length TUC338 transcript sequences (Braconi et al., 2011) or truncated cDNA fragments into pcDNA3.1 vector using BamHI and EcoRI sites. The following primers were used: for full-length TUC338 (forward primer: 5'- CGCGGAT-CCAGTGGGCTCTGTAGGGGTTCAAC, reverse primer: 5'- CCGGAATTCGTTGGTGTTAC-CATCTGGTGGGC); for TUC338/1-115 (forward primer: 5'-CGCGGATCCAGTGGGCTCTGTA-GGGGTTCAAC, reverse primer: 5'-CCGGAATTCAGATTTCACACTGCACAATTGGGC); for TUC338/116-237 (forward primer: 5'-CGCGGATCCGCCACTAGGTAACTTTTTTTT, reverse primer: 5'-CCGGAATTCCCAGCA-TGAAATTCACACAAA); for TUC338/238-354 (forward primer: 5'-CGCGGATCCTGACAAGGTGCCGGATTGACA, reverse primer: 5'-CCGGAATTCAGG-CACATGGACGGGGTGGTG); for TUC338/355-460 (forward primer; 5'-CGCGGATCCCAA-CCCTGACCTGGAGGGAC, reverse primer: 5'-CCGGAATTCGCCCCCCGTGTGTTGGCAGT); for TUC338/461-575 (forward primer: 5'-CGCGGATCCCAGTGGCGCTGGTGATTTTTG, reverse primer: 5'-CCGGAATTCGTTGG-TGTTACCATCTGGTGGGC). The constructs were linearized using EcoRI and served as templates for *in vitro* transcription. RNA probes was synthesized by T7 polymerase (Promega, Madison, WI) and labeled at 3' end with biotin using RNA 3' End Biotinylation Kit (Thermo Scientific, Rockford, IL).

Cell extracts were prepared from HepG2 cells by suspension in cell extract buffer (50mM Tris pH8.0, 50mM NaCl, 1mM PMSF, 1mM DTT, protease inhibitor cocktail), followed by three freeze-thaw cycles, and passage through 20 and 30-gauge needles. Extracts were pre-cleaned by incubating with Dynabeads M-280 streptavidin for 30 minutes to remove endogenous biotin. The pre-cleaned cell extract was then incubated with biotin-labeled RNA probes for 30 minutes in binding buffer [100mM HEPES pH7.3, 200mM KCl, 10mM $MgCl_2$, 10mM DTT, 2U SUPERase-in (Ambion, Austin, TX)]. For competition assays, pre-cleaned cell extract was pre-incubated with unlabeled TUC338 RNA or anti-PAI-RBP1 antibody (Abnova, Taiwan) for 30 minutes before the addition of the Biotin-labeled RNA probe. The binding mixtures were mixed with 1x Novex Hi-density TBE sample buffer (Life Technologies, Grand Island, NY) loaded onto a 6% DNA retardation gel (Life Technologies, Grand Island, NY) and electrophoresed in 0.5X TBE buffer at 100V. Gels were then transferred to a Hybond-N+ nylon membrane (GE Healthcare Life Sciences, Piscataway, NJ). The membrane was crosslinked and then incubated with IRDy1800CW-streptavidin antibody (LI-COR Biosciences, Lincoln, NE). RNA was visualized using the LI-COR Odyssey infrared imaging system (LI-COR Bioscience, Lincoln, NE).

Reporter constructs and luciferase assay.

For p53 assays, cells were transfected with negative control or siRNA to TUC338 using lipofectamine 2000, and 24 hours later with 800ng of p53-luc reporter containing firefly luciferase and pRL-TK Renilla luciferase expression constructs. For PAI-1 3'UTR reporter constructs, the 3'UTR of PAI-1 was cloned downstream of the firefly luciferase gene of pGL3 control vector using XbaI site. Total complementary DNA was obtained by reverse-transcription using Iscript RT kit (Bio-Rad Laboratories, Hercules, CA). The 3'UTR of PAI-1 was amplified using the following primers: for PAI-13U (F: 5'-CTAGTCTAGACCCTGGGGAAAGACGCCTTCATC, R: 5'-GCTCTAGAGTCCTGACATATT-

CTTCGTATTTAT); for PAI-13US (F: 5'-CTAGTCTAGACCCTGGGGAAAGACGCCTTCATC, R: 5'-GCTCTAGAGCGAGTTTAAATA-ATATTATTTTCC). HepG2 cells were co-transfected with pGL3-PAI-1 3'UTR and pRL-TK Renilla luciferase expression constructs. Cell extracts were assayed for luciferase activity using Dual Glo Assay system (Promega, Madison, WI) and a multiwall plate luminometer (Turner Biosystems, Sunnyvale, CA).

Cell Growth Assays.
For anchorage-dependent cell growth, HepG2 cells were seeded into 96-well plates (5,000 per well) 24 hours post-transfection, and proliferation assessed using CellTiter 96 AQueous cell proliferation assay kit (Promega, Madison, WI). The proliferation index calculated as the percentage of the corrected absorbance at 490nm in gene-specific siRNA to NT control siRNA transfectants. For anchorage-independent cell growth, HepG2 cells were plated 24-hours after transfection using a 2-layer agar system, in which the final concentrations of agar were 0.6% and 0.4% in the bottom and top layers, respectively. Cells were plated in 96-well plates (600 cells per well), and anchorage independent cell growth was fluorometrically assayed after 7 days using alamarBlue (Life Technologies, Grand Island, NY). Final values were obtained by subtracting background fluorescence values from wells without cells. For colony forming studies, cells (1250 cells per well) were also plated in 24-well plates. After 4-week incubation cell colonies were fixed using 100% methanol and stained using Giemsa. Stained cell colonies were counted under a microscope.

Statistical analysis.
Data are expressed as the mean ± standard error of the mean (SE). Comparisons between groups were performed with the two-tailed Student's *t* test. Significance was accepted when $P<0.05$.